Performance Evaluation of an Induction Motor Drive with Direct Torque Control for Open-End Winding and Cascaded Three-Level Topologies

S.V. Siva Prasad
sivaprasadsatelli@gmail.com

Rajendra Singh R.
rsrathore2007@gmail.com

V.T. Somasekhar
sekhar@nitw.ac.in

Suresh Lakhimsetty
suresh.201@gmail.com

Department of Electrical Engineering
National Institute of Technology Warangal
Warangal, INDIA

***Abstract* - The advantages of using Direct Torque control (DTC) vis-à-vis Volt/Hz and Field Oriented Control (FOC) for the control of Induction Motor are well documented in the literature. It is also fairly well known that the performance of any AC motor drive is enhanced, when it is fed with multilevel inverters compared to the conventional two-level inverters. In this paper, the results of comparative analyses are reported when an induction motor is driven with 3-level inverters realized by (i) a three-level Cascaded Inverter and (ii) a dual-inverter driven Open-End Winding configuration. The performance indices considered are: a) THD in current b) flux-ripple and c) torque-ripple. To assess the benefit obtained by the employment of each approach, the results are compared with the performance of a 2-level Voltage Source Inverter employing classical DTC.**

Keywords: Cascaded Inverter; DTC; Multilevel Inverter; Torque ripple; OEWIMD

I. Introduction

Variable speed Induction Motor (IM) drives are widely used in the applications such as fans, blowers, elevators, electric vehicles, air conditioning systems, marine systems etc. [1]. Economical and efficient speed control of IM drive is achieved by using the frequency controlled Voltage Source Inverters (VSIs). Field Oriented Control (FOC) and Direct Torque Control (DTC) are the most popularly used control strategies for variable speed, high performance IM drives. The drawbacks associated with the FOC scheme are: i) knowledge of the machine parameters for the estimation of flux and electromagnetic torque ii) employment of current controllers and iii) reference frame transformation [2].

On the other hand, DTC merely requires the knowledge of the stator resistance for the estimation of flux and electromagnetic torque. DTC scheme is very simple to implement, as it eliminates the need of current controllers and the reference frame transformation. Arguably, it results in a better dynamic response compared to the FOC [3].

DTC can be implemented using either 2-Level (2-L) or Multilevel Inverters (MLI). From the perspective of inversion compared to the 2-L VSI, the employment of MLIs results in lower THD in voltage and current. It is obvious that, the reduced THD in current would result in the reduction of flux and torque ripple.

There are several contending power circuit configurations for MLIs. Popular amongst these are: i) the Neutral Point Clamped (NPC) configuration ii) the Flying Capacitor (FC) configuration and iii) the Cascaded H-Bridge (CHB) configuration. Abundant literature is available regarding the applicability, performance and limitations of each of these topologies [4, 5]. Several PWM strategies were also suggested for each of these MLIs [6].

The concept of dual-inverter fed Open-End Winding Induction Motor Drives (OEWIMD) is relatively new. Unlike the other topologies, wherein the motor constitutes the “load” for the MLI as a separate entity, it is an integral part of the OEWIMD. OEWIMDs too realize several levels like other topologies [7, 8], though a 3-level topology is selected in the present study.

Another configuration, known as the Cascaded 3-Level (C3-L) inverter was proposed, wherein 3-level inversion is achieved by the cascaded connection of two existing 2-level inverters [9] as a retrofit solution. This configuration is also amenable for realizing more than 3-levels [10].

It’s a foregone conclusion that an IM, employing any of the aforementioned 3-level VSIs, would yield a better performance compared to the conventional 2-level VSI. However, their relative performance vis-à-vis the 2-level VSI have not been quantified in the past. It is this gap this paper intends to fill.

In this paper, the performance evaluation is carried out for the C3-L VSI and the OEWIMD topology. In both of these cases, the motor is controlled with the classical DTC technique. To facilitate a better visualization, the performance of these three-level (3-L) VSIs are compared with the performance of the conventional 2-level VSI, which is taken as the benchmark. The performance indices such as ripple in the electromagnetic torque, flux, THD in current are considered to evaluate the performance of the IM DTC drive.

II. Three-Level Inverter Topologies

A. Dual inverter fed OEWIM topology

Three-level inversion can be obtained when open stator windings are fed by two two-level inverters (the dual-inverter system) from either end as shown in Fig.1. Each inverter of the dual-inverter system is fed by an isolated DC power supply to

978-1-5090-4874-8/17/$31.00 ©2017 IEEE

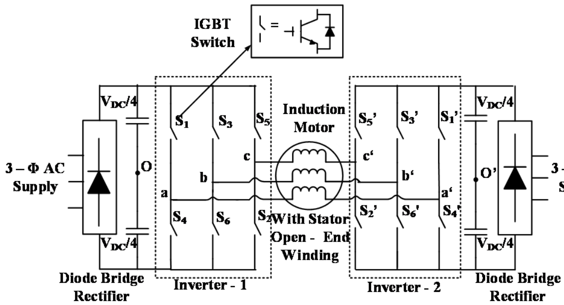

Fig. 1. Three – level OEWIMD

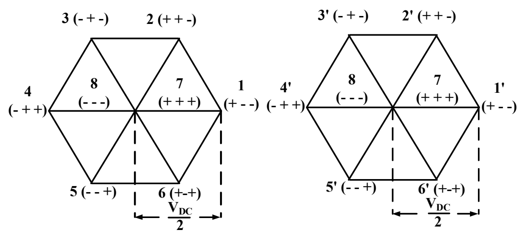

Fig.2. Individual space vector diagrams

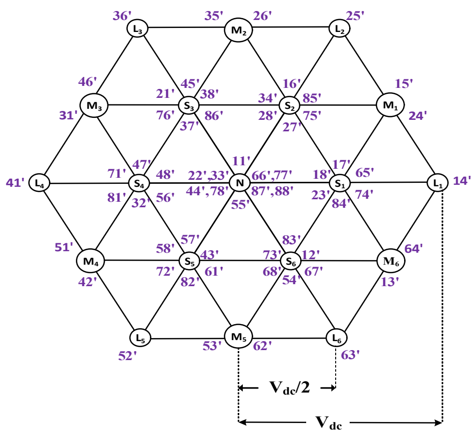

Fig. 3. Resultant space vector diagram of OEWIMD

ensure the blockage of zero-sequence currents. The individual inverter states as well as the dual-inverter system are shown in Fig. 2 and Fig. 3 respectively. As each of the constituent 2-L VSIs has 8 (Fig.2), the resultant dual-inverter system would have 64 (8x8) space vector combinations as shown in Fig.3 [11].

The relationship between the phase voltage and pole voltage of OEWIMD and their expressions are detailed given in [12]. The phase voltage across the OEWIMD in terms of pole voltage can be written as,

$$\begin{bmatrix} v_{aa'} \\ v_{bb'} \\ v_{cc'} \end{bmatrix} = \frac{V_{DC}}{6} \begin{bmatrix} 2 & -1 & -1 \\ -1 & 2 & -1 \\ -1 & -1 & 2 \end{bmatrix} \begin{bmatrix} v_{ao} - v_{a'o'} \\ v_{bo} - v_{b'o'} \\ v_{co} - v_{c'o'} \end{bmatrix} \quad (1)$$

B. Cascaded 3-Level (C3-L) Inverter topology

Fig. 4 shows the cascaded 3-level inverter topology, which is realized by retrofitting two existing 2-L VSIs by connecting them in a cascaded manner. Fig.2 indicates the switching states of the constituent 2-L VSIs of the C3-L inverter also. The resultant space vector diagram for the C3-L VSI is shown in Fi-

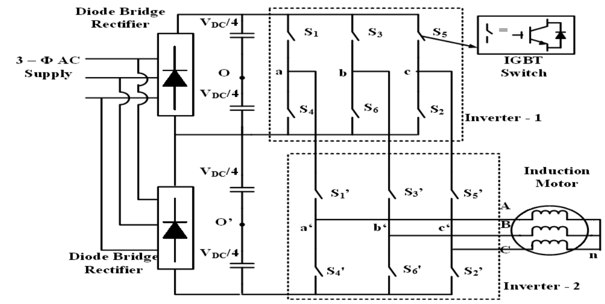

Fig.4. Three- Level Cascaded Inverter Topology

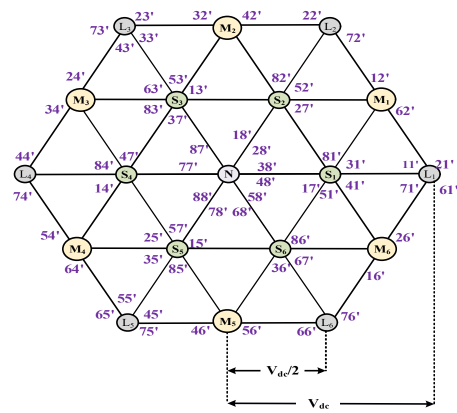

Fig.5. Resultant space vector diagram of C3-L Inverter

g. 5. Fig. 3 and Fig. 5 reveal that, both power circuits offer identical space-vector combinations. However, the distribution of space vector combinations over these locations is very different for these two power circuit configurations. While the disposition of the space vector combinations is symmetrical for the OEWIMD configuration, it is highly unsymmetrical in the case of the C3-L VSI. The phase voltage across the IM drive in terms of pole voltage can be written as,

$$\begin{bmatrix} v_{An} \\ v_{Bn} \\ v_{Cn} \end{bmatrix} = \frac{V_{DC}}{3} \begin{bmatrix} 2 & -1 & -1 & 4 & -2 & -2 \\ -1 & 2 & -1 & -2 & 4 & -2 \\ -1 & -1 & 2 & -2 & -2 & 4 \end{bmatrix} \begin{bmatrix} s_4 \&\& s_{1'} \\ s_6 \&\& s_{3'} \\ s_4 \&\& s_{5'} \\ s_1 \&\& s_{1'} \\ s_3 \&\& s_{3'} \\ s_5 \&\& s_{5'} \end{bmatrix} (2)$$

III. REVIEW OF CLASSICAL DTC WITH 2-L VSI

The concept of DTC of IMs is well known, it is briefly reviewed in this section. The torque expression for induction motor can be expressed in vector form as,

$$\overline{m_e} = \frac{2}{3}\frac{P}{2}\frac{L_m}{L_r L_s'}\left|\overline{\psi_s}\right|\left|\overline{\psi_r}\right| \sin\gamma \quad (3)$$

Where ψ_s and ψ_r are the stator and rotor flux vectors (both fixed to the stationary reference frame), L_m is the magnetizing inductance, $L_s{}'$ is a measure of the stator inductance, L_r is the rotor inductance, P is the number of poles and γ is the angle between the stator and rotor fluxes. If the rotor flux remains constant, the incremental torque depends on the change in the stator flux, which in turn depends on the stator voltage and the corresponding change in the angle δ. The expression for incremental torque is given as

$$\overline{\Delta m_e} = \frac{2}{3}\frac{P}{2}\frac{L_m}{L_r L_s'}\left|\overline{\psi_r}\right|\left|\overline{\psi_s} + \Delta\overline{\psi_s}\right| \sin\Delta\gamma \tag{4}$$

The block diagram representation of the conventional DTC is shown in Fig. 6, it mainly consists of flux and torque estimator block, where the electromagnetic torque and flux are estimated in the stationary frame of reference by using the following equations,

$$m_d = \frac{2}{3}\frac{P}{2}\left(\psi_{ds} i_{qs} - \psi_{qs} i_{ds}\right) \tag{5}$$

$$\psi_s = \sqrt{(\psi_{ds})^2 + \left(\psi_{qs}\right)^2} \tag{6}$$

Where, ψ_{ds} and $\psi_{qs}$are the *d-q* components of the stator flux and i_{ds}, i_{qs} are the *d-q* axis components of the motor phase current.

IV. CONVENTIONAL DTC FOR THREE – LEVEL TOPOLOGIES

The principle of conventional DTC for 2-L VSI is extended to the OEWIMD and C3-L inverter fed IM drive and their block diagrams are shown in Figs. 7 & 8. Both of these three-level topologies use a 2-level flux hysteresis controller and a 7-level torque hysteresis controller. As explained earlier, both OEWIMD and C3-L inverter topologies have a total of 64 space vector combinations spread over 19 space vector locations. These 19 space vector locations are grouped into the following categories: i) null vector (*N*), ii) small vectors (S_x), iii) medium vectors (M_x) and iv) large vectors (L_x), where $x \epsilon$ (1, 2, 3, 4, 5 & 6) as shown in Figs. 3 & 5. The look up tables used for the selection of voltage vectors in the case of the OEWIMD and the C3-L topologies are shown in Tables I & II respectively.

V. SIMULATION RESULTS & COMPARATIVE STUDY

The simulation results are presented in this section to evaluate the relative performance of the three-level inverter topologies with the 2-L VSI. Conventional DTC is employed in all the three cases to facilitate a fair comparison. Fig. 9 shows the performance of the IM with DTC employing the 2-L VSI, wherein the speed command signal is varied from 0 to 1200 RPM (mode of acceleration) and then to -1200 RPM (mode of speed reversal). It may be seen that the speed command is well obeyed (Fig. 9(a)). The developed electromagnetic torque is shown in Fig.9 (b). Figures 9(c) shows the stator voltage applied to the motor, while Fig. 9(d) shows the back-emf developed across the magnetizing inductance, which is obtained by subtracting the voltage across the leakage inductance associated with the stator. The zoomed view of the stator current is presented in Fig. 9(e), which is sinusoidal with the switching ripple superposed on it. It may be noted that the torque is non-zero only during the time of acceleration and the speed reversal.

Similar responses are shown for the three-level inverter fed IM drive with DTC in Fig. 10 (for OEWIMD) and Fig.11 (for the C3-L VSI) respectively. It may be observed that, while the applied voltage to the stator shows a fair amount of arbitrariness, owing to the random switching action of the power semi-conductor devices of the inverter, the back-emf waveform is periodic owing to both electrical and mechanical inertias.

TABLE I: LOOK UP TABLE FOR SELECTION VOLTAGE VECTORS

Flux Err Status	Torque Err Status	Sector Number					
		S_1	***S_2***	***S_3***	***S_4***	***S_5***	***S_6***
1	3	L_2	L_3	L_4	L_5	L_6	L1
	2	M_2	M_3	M_4	M_5	M_6	M_1
	1	S_2	S_3	S_4	S_5	S_6	S_1
	0	N	N	N	N	N	N
	-1	S_6	S_1	S_2	S_3	S_4	S_5
	2	M_6	M_1	M_2	M_3	M_4	M_5
	-3	L_6	L_1	L_2	L_3	L_4	L_5
-1	3	L_3	L_4	L_5	L_6	L_1	L_2
	2	M_3	M_4	M_5	M_6	M_1	M_2
	1	S_3	S_4	S_5	S_6	S_1	S_2
	0	N	N	N	N	N	N
	-1	S_5	S_6	S_1	S_2	S_3	S_4
	-2	M_5	M_6	M_1	M_2	M_3	M_4
	-3	L_5	L_6	L_1	L_2	L_3	L_4

Fig. 12 shows the FFT analysis of the no-load current of the three DTC configurations at a speed of 900 RPM. It can be observed that the spectral performance is better in 3-L topologies as compared to the 2-L VSI. Fig. 13 shows the flux-ripple associated with the three candidate configurations. It may be observed that, there is no advantage of resorting to the use of three-level inverters compared to the 2-L VSI. This is an expec-

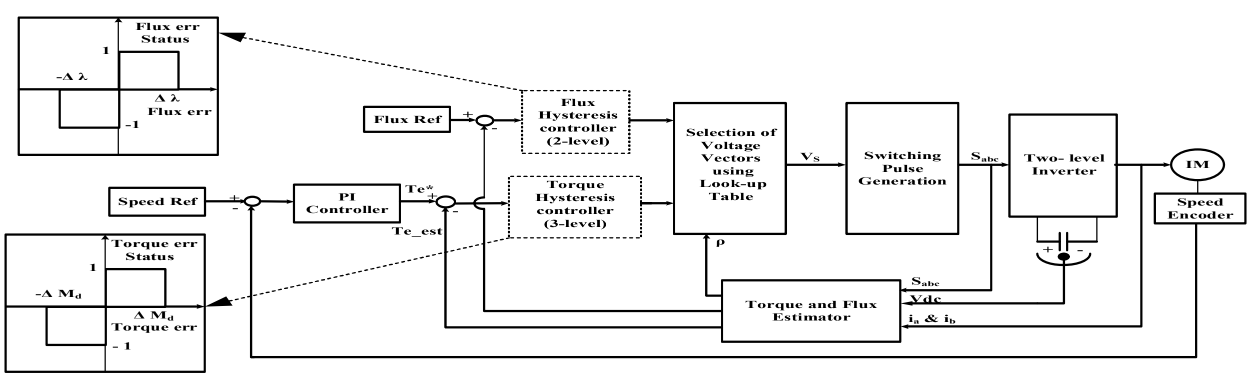

Fig.6. Block Diagram of 2-L VSI DTC

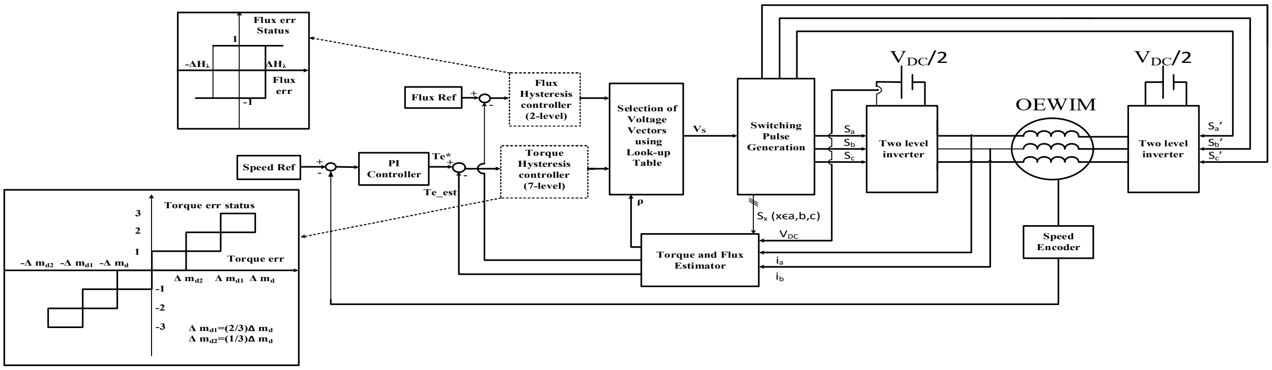

Fig.7. Block Diagram of OEWIMD with DTC

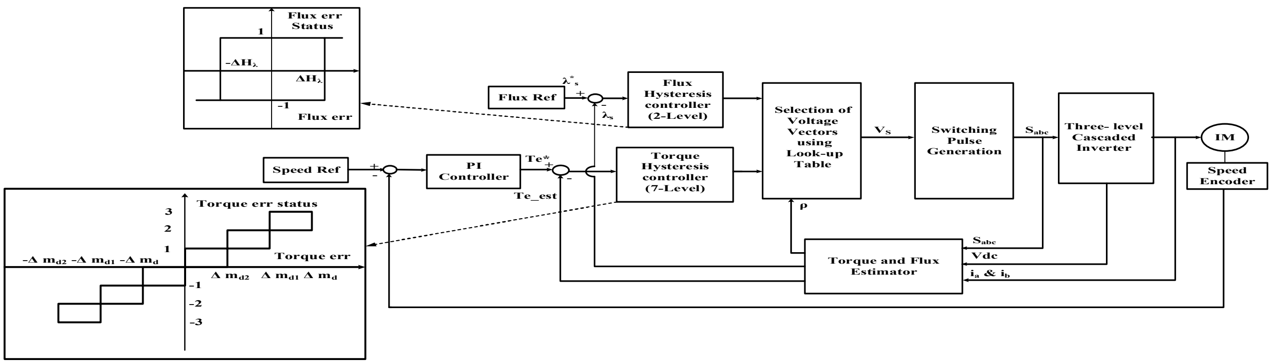

Fig.8. Block diagram of C3-L inverter fed IM with DTC

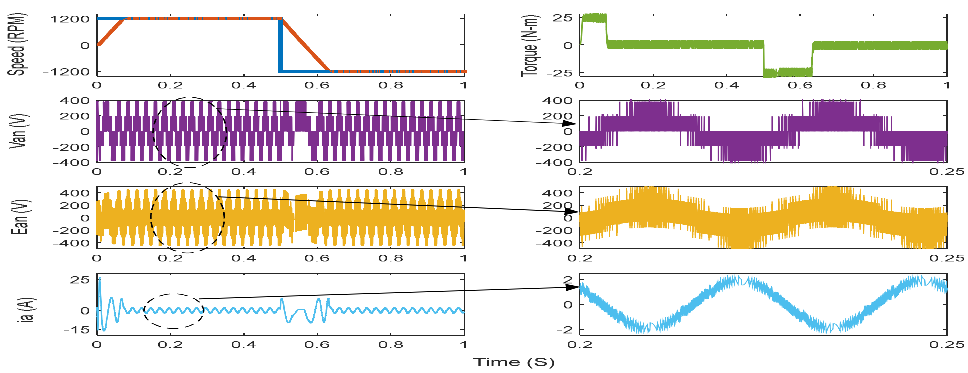

Fig. 9. 2-L VSI DTC (a) speed reversal (b) Electromagnetic Torque (T_e) (c) Stator Phase A voltage (d) Rotor Phase A voltage (e) stator Phase A current

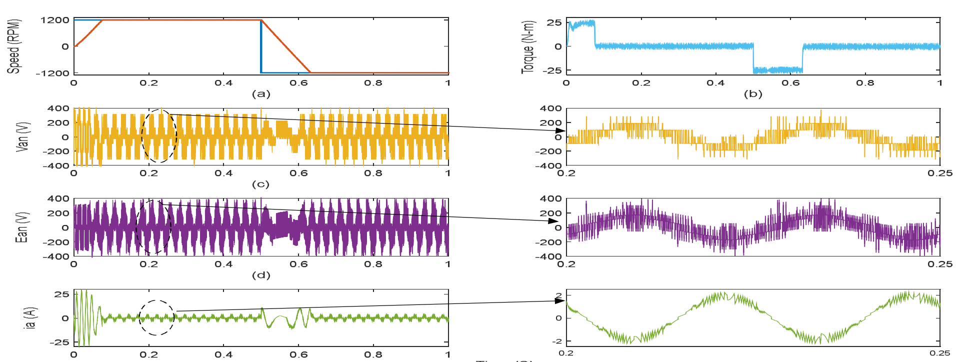

Fig. 10. 3-L OEWIMD DTC (a) speed reversal (b) Electromagnetic Torque (T_e) (c) Stator Phase A voltage (d) Rotor Phase A voltage (e) stator Phase A current

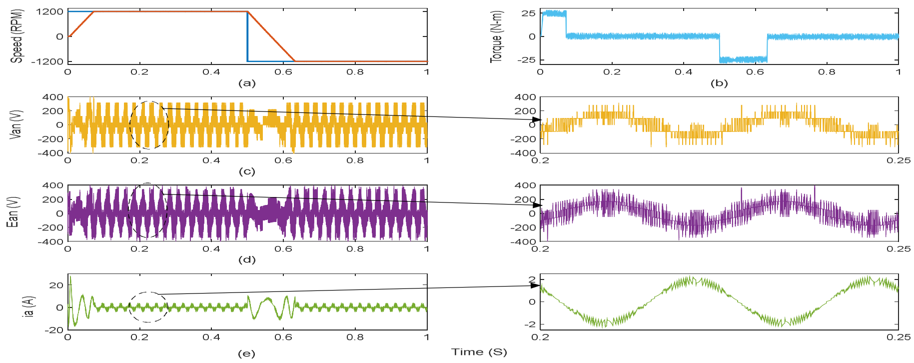

Fig. 11. C3-L inverter DTC (a) speed reversal (b) Electromagnetic Torque (T_e) (c) Stator Phase A voltage (d) Rotor Phase A voltage (e) stator Phase A current

TABLE II: LOOK UP TABLE FOR SELECTION VOLTAGE VECTORS

Flux Err Status	Torque Err Status	Sector Number											
		S_1	S_2	S_3	S_4	S_5	S_6	S_7	S_8	S_9	S_{10}	S_{11}	S_{12}
1	3	L_3	L_3	L_4	L_4	L_5	L_5	L_6	L_6	L_1	L_1	L_2	L_2
	2	M_2	M_3	M_3	M_4	M_4	M_5	M_5	M_6	M_6	M_1	M_1	M_2
	1	S_3	S_3	S_4	S_4	S_5	S_5	S_6	S_6	S_1	S_1	S_2	S_2
	0	N	N	N	N	N	N	N	N	N	N	N	N
	-1	S_5	S_5	S_6	S_6	S_1	S_1	S_2	S_2	S_3	S_3	S_4	S_4
	-2	M_4	M_5	M_5	M_6	M_6	M_1	M_1	M_2	M_2	M_3	M_3	M_4
	-3	L_5	L_5	L_6	L_6	L_1	L_1	L_2	L_2	L_3	L_3	L_4	L_4
-1	3	L_2	L_2	L_3	L_3	L_4	L_4	L_5	L_5	L_6	L_6	L_1	L_1
	2	M_1	M_2	M_2	M_3	M_3	M_4	M_4	M_5	M_5	M_6	M_6	M_1
	1	S_2	S_2	S_3	S_3	S_4	S_4	S_5	S_5	S_6	S_6	S_1	S_1
	0	N	N	N	N	N	N	N	N	N	N	N	N
	-1	S_6	S_6	S_1	S_1	S_2	S_2	S_3	S_3	S_4	S_4	S_5	S_5
	-2	M_5	M_6	M_6	M_1	M_1	M_2	M_2	M_3	M_3	M_4	M_4	M_5
	-3	L_6	L_6	L_1	L_1	L_2	L_2	L_3	L_3	L_4	L_4	L_5	L_5

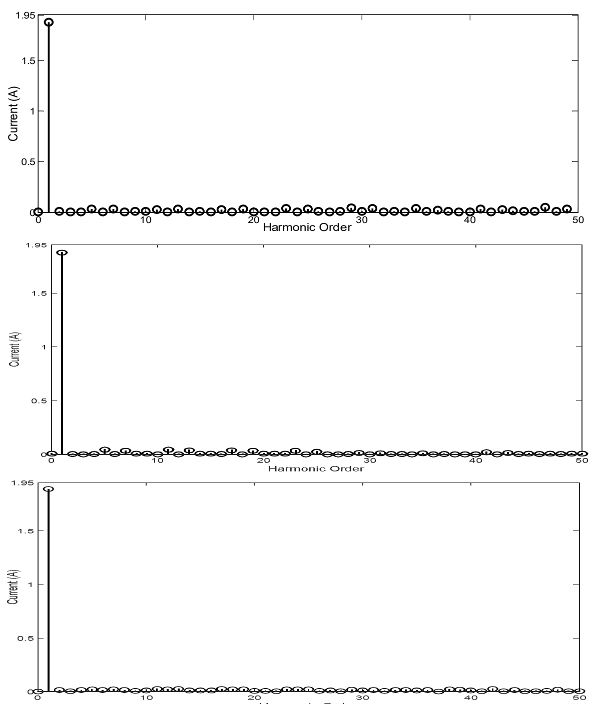

Fig. 12. Current FFT Analysis: 2-L VSI DTC (top) 3-L OEWIMD DTC (middle) C3-L inverter DTC (bottom)

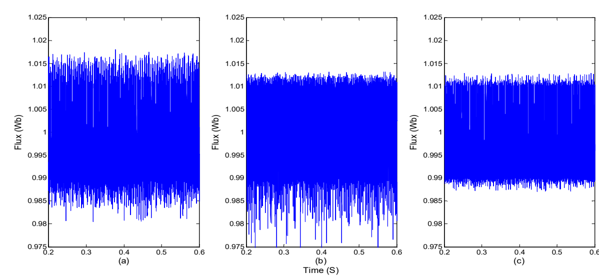

Fig. 13. Flux ripple (a) 2-L VSI DTC (b) 3-L OEWIMD DTC (c) C3-L inverter DTC

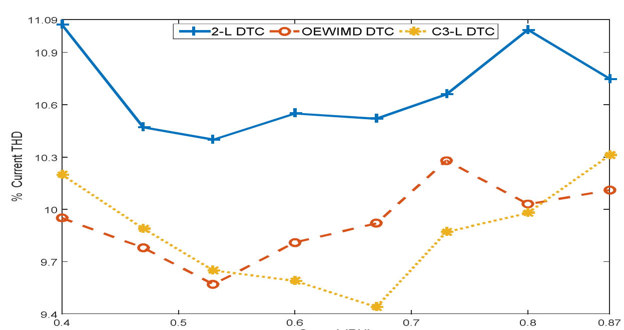

Fig. 14. Current THD Comparison

ted result on account of the high electrical inertia associated with the magnetizing inductance of the IM. However, the currents drawn by the motor could be considerably different and the use of three-level inverters are well justified. Fig. 14 show the THD in the stator currents for the three power circuit configurations at no-load. It is evident that the three-level inverters perform considerably better compared to the 2-L VSI.

Fig. 15 shows the ripple in the electromagnetic torque for the three cases and the quantitate performance among the three DTC topologies in terms of ripple in torque error is shown in Table III. It is evident that the torque ripple with both of the 3-level inverters is considerably lower compared to the one obtained with the 2-L VSI. This is the direct consequence of the lower THD in the stator currents of the IM.

Fig. 16 shows the variation of the stator current and torque developed for all the three power circuit configurations under varying load conditions.

TABLE III: QUANTITATIVE PERFORMANCE

Speed (RPM)	**Ripple in Torque error**		
	2-L VSI DTC	***3-L OEWIMD DTC***	***C3-L inverter DTC***
300	0.438	0.187	0.188
600	0.598	0.372	0.373
900	0.740	0.561	0.562
1200	0.822	0.745	0.747
1500	1.105	0.935	0.936

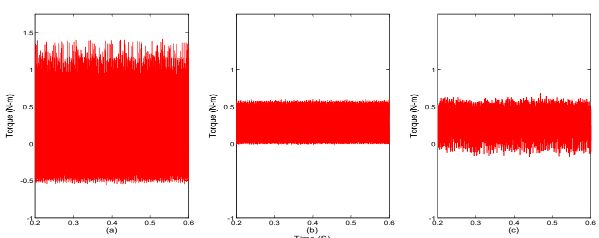

Fig. 15. Torque ripple (a) 2-L VSI DTC (b) 3-L OEWIMD DTC (c) C3-L inverter DTC

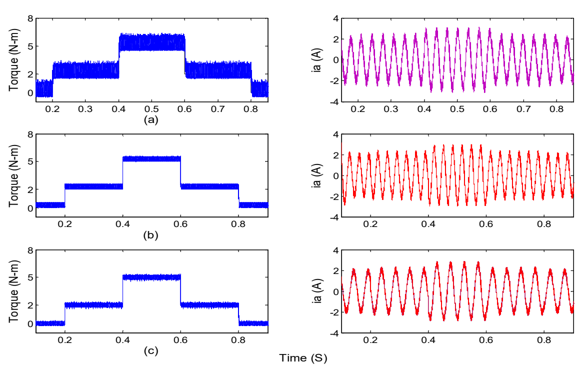

Fig. 16. Load torque with phase-A current (a) 2-L VSI DTC (b) 3-L OEWIMD DTC (c) C3-L inverter DTC

VI. CONCLUSIONS

In this paper, a comparative evaluation is performed between the three-level OEWIMD and the C3-L VSI, employing the conventional DTC technique. To visualize the benefit reaped by the use of these three-level VSIs clearly, their performance with DTC is compared to that of the one obtained with the 2-L VSI. The simulation studies indicate that there is an improvement in the current THD and the torque ripple when three-level inverters are used. Amongst the three-level inverters, the C3-L VSI registers a better performance in middle range of speed, as compared to the three-level OEWIMD.

REFERENCES

[1] S. Kouro, J. Rodriguez, W. Bin, S. Bernet, and M. Perez, "Powering the future of industry: High-power adjustable speed drive topologies," *IEEE Ind. Appl. Mag*., vol. 18, no. 4, pp. 26–39, Jul./Aug. 2012.

[2] I. Takahashi and T. Noguchi, "A New Quick-Response and High Efficiency Control Strategy of an Induction Motor," , *IEEE Trans. Industry Applications*, vol. IA-22, pp. 820-827, 1986.

[3] Domenico Casadei, Francesco Profumo, Giovanni Serra, and Angelo Tani "FOC and DTC: Two Viable Schemes for Induction Motors Torque Control" *IEEE Trans. Power Electron*, Vol. 17, No. 5, pp. 779-789, Sep. 2002.

[4] Viju Nair R, Arun Rahul S, R. Sudharshan Kaarthik, Abhijit Kshirsagar, and K. Gopakumar "Generation of Higher Number of Voltage Levels by Stacking Inverters of Lower Multilevel Structures With Low Voltage Devices for Drives" *IEEE Trans. Power Electron.,* vol. 32, no. 1, pp. 52-59, Jan. 2017.

[5] Krishna Kumar G., Alekh Ranjan, Pallavee Bhatnagar, Lalit Kumar S, and Shailendra Jain "Multilevel Inverter Topologies With Reduced Device Count: A Review" *IEEE Trans. Power Electron*., vol. 31, no. 1, pp.135 – 151, Jan. 2016.

[6] Jackson Lago, Marcelo Lobo Heldwein, "Generalized Synchronous Optimal Pulsewidth Modulation for Multilevel Inverters" *IEEE Trans. Power Electron.*, Vol. 32, Issue: 8, pp. 6297-6307, Aug. 2017.

[7] K. Ramachandra Sekhar and S. Srinivas "Discontinuous Decoupled PWMs for Reduced Current Ripple in a Dual Two-Level Inverter Fed Open-End Winding Induction Motor Drive" *IEEE Trans. Power Electron.*, vol. 28, no. 5, pp. 2493-2502, May 2013.

[8] Barry Venugopal Reddy, Veeramraju Timurala Somasekhar, and Yenduri Kalyan "Decoupled Space-Vector PWM Strategies for a Four-Level Asymmetrical Open-End Winding Induction Motor Drive With Waveform Symmetries" *IEEE Trans. Ind. Electron.,* vol. 58, no. 11, pp. 5130 - 5141, Nov. 2011.

[9] V.T. Somasekhar and K. Gopakumar "Three-level inverter configuration cascading two two-level inverters" *IEE Proc.-Eleclr. Power Appl*, Vol. 150, No. 3, May 2003.

[10] M.R. Baiju, K. Gopakumar, V.T. Somasekhar, K.K. Mohapatra & L. Umanand "A Space Vector Based PWM Method Using Only the Instantaneous Amplitudes of Reference Phase Voltages for Three Level Inverters" *EPE Journal,* Vol. 13, no.2, May 2003.

[11] S. Srinivas ; V.T. Somasekhar "Space-vector-based PWM switching strategies for a three-level dual-inverter-fed open-end winding induction motor drive and their comparative evaluation" *IET Electric Power Applications*, Vol: 2, Issue: 1, pp. 19-31, Jan. 2008.

[12] Suresh Lakhimsetty, Nagarjun Surulivel and V.T.Somasekhar "Improvised SVPWM Strategies for an Enhanced Performance for a Four-Level Open-End Winding Induction Motor Drive" *IEEE Trans. Ind. Electron*., vol. 64, no. 4, pp. 2750-2759, Apr. 2017.